(Preprint) AAS 25-190

INCREASING THE ELECTROSTATIC FORCE BETWEEN SPACECRAFT USING A PULSED ELECTRON BEAM

Amy Haft* **and Hanspeter Schaub†**

The electrostatic tractor is a concept for debris removal in Geosynchronous Earth Orbit (GEO) in which a servicer spacecraft aims an electron gun at a target debris object. The electron emission from the servicer causes it to charge positively, while the impact of the electrons cause the target to charge negatively. A voltage equilibrium is achieved in balance with the ambient space environment current. The result is an attractive electrostatic force between the spacecraft that allows the servicer to re-orbit a tumbling debris object into a graveyard orbit. Previous studies have shown that this electrostatic force is on the order of milli-Newtons, causing the time to achieve the required ΔV to successfully re-orbit to be several months. However, these studies used a continuous electron beam (e-beam) current. This paper studies how using a pulsed e-beam, for a given mean power level, can increase the attractive electrostatic force between the servicer and the target if sufficient current can be applied. In addition, there is a space-weather dependent optimal duty cycle such that the force is strongest. Enhancing the electrostatic force can decrease the re-orbit time by orders of magnitude, with even better performance when using stronger e-beam parameters. This paper looks at the effects of the changing GEO environment on pulsed e-beam performance.

INTRODUCTION

Spacecraft in high Earth orbit are known to charge naturally due to currents from the local plasma, such as ambient electron and ion currents or the photoelectron current when in sunlight [1, Chapter 1]. Due to the rarified and energetic nature of the plasma at high altitudes, such as Geosynchronous Earth Orbit (GEO), spacecraft may charge to severe negative potentials on the order of thousands to tens of thousands of volts in eclipse.[2] The ATS-6 satellite experienced record charging up to -19keV in GEO.[3] While spacecraft charging often is regarded as bothersome due to risks of deep dielectric discharge and differential charging, previous studies show that active spacecraft charging at high altitudes can be employed as a means of re-orbiting defunct satellites[4–6] or detumbling spacecraft.[7–11] Active spacecraft charging refers to the use of a non-natural current, commonly an electron gun, from a servicer spacecraft onto a target object in order to control the potential of both spacecraft and generate forces between them. GEO is a suitable environment for active charging because the Debye length, a measure of how far a charged object's electrostatic effect persists, is on the order of hundreds of meters, compared to centimeters in Low Earth Orbit (LEO).[12]

The proposed method of re-orbiting space debris is the Electrostatic Tractor (ET).[4] Here, a servicer spacecraft equipped with an ancillary propulsion system uses an electron beam (e-beam) to

*Graduate Research Assistant, Ann and H.J. Smead Department of Aerospace Engineering Sciences, Colorado Center for Astrodynamics Research, AIAA Student Member, Email: amy.haft@colorado.edu.

†Distinguished Professor and Department Chair, Schaden Leadership Chair, Ann and H.J. Smead Department of Aerospace Engineering Sciences, Colorado Center for Astrodynamics Research. AAS Fellow, AIAA Fellow.

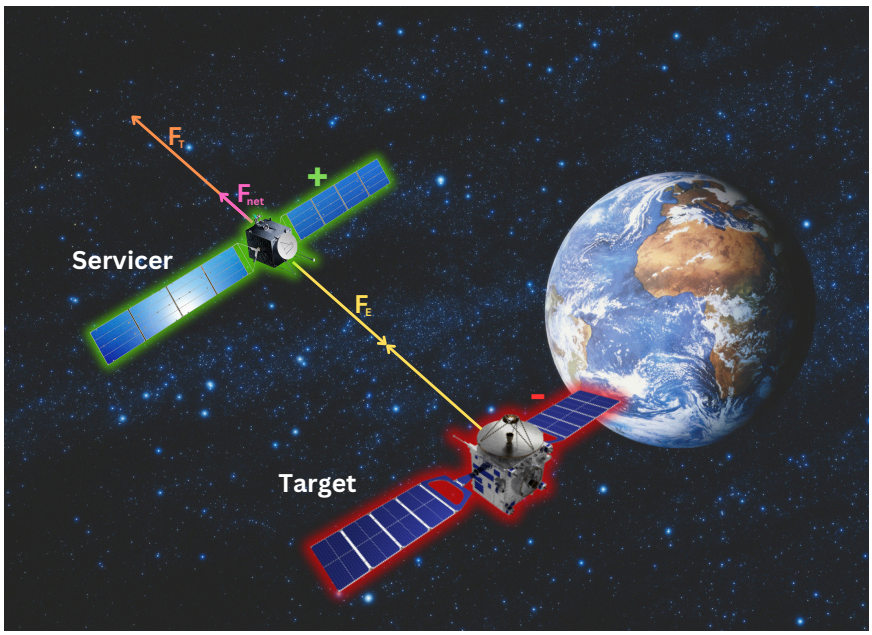

Figure 1: Electrostatic tractor concept with forces visualized

make the potential of a target object negative while its own potential becomes increasingly positive. Eventually, the positive potential of the servicer becomes large enough such that some electrons are attracted back to the servicer and the currents on both the servicer and target reach a net zero state. The electric potential of a spacecraft when the net current is zero is the equilibrium potential. An attractive force that allows the servicer to re-orbit the target results. The servicer's propulsion system must then provide the inertial force to achieve the necessary change in velocity ΔV to put both spacecraft onto a transfer orbit and then into the final graveyard orbit.

To maintain the electrostatic force between spacecraft, the thrust force provided by the propulsion system cannot be significantly larger than the electrostatic force. Thus, it is helpful for mission efficiency to maximize the electrostatic force. Previous research used a continuous e-beam to calculate the electrostatic force.[13,14] In some studies, the e-beam parameters were varied for a range of plasma conditions to find the optimal combination of beam energy and current to maximize the e-tractor force.[15,16] In contrast, Reference 17 investigated if a pulsed e-beam can result in an increase in force.[17] The theory predicted that, for a given power level, it is possible to achieve higher spacecraft potentials by turning the e-beam on for only a fraction of the time. This technique would cause the e-beam current and voltage to be increased relative to the duty cycle to achieve the same average power level. Because the force increases as a function of spacecraft potential, the pulsed beam theoretically can result in a higher electrostatic force than a continuous beam.

The study conducted in References 17 and 18 presents an interesting baseline for the pulsed beam concept. While results show that the pulsed beam can increase the force, the effect is not optimized as a function of the duty cycle. Instead, the authors focus on optimizing the electrostatic force by varying the tuning parameter, which determines the ratio of e-beam current to e-beam voltage. The effect of local time during quiet conditions is also observed, and storm conditions are looked at for specific parameters. The e-beam is tested only at duty cycles of 10%, 25%, 50%, and 100% (continuous case). As a result, the full effect of the power-limited pulsed e-beam is

not recognized. The study also does not account for multiple populations of plasma particles in the GEO environment, instead only using a single-Maxwellian distribution of particles. The GEO environment plays a significant role in the effectiveness of the ET, so it is necessary to build upon this work with an increasingly realistic model.

The purpose of this research is to employ the coupled spacecraft effects to determine if there exists an optimal duty cycle such that the electrostatic force is maximized. Of interest is investigating if new emerging electron guns with high currents and rapid response times could lead to a better power constrained e-tractor performance. For example, Think Orbital is developing a novel space-based welding system that can sustain high currents and has fast response times.* A key concern is that it takes a finite time for space objects to charge which is a function of the e-beam properties and the local space environment. If the charging time is too long compared to the pulsed beam on-time then the forces would be small. The charging simulations are conducted using a bi-Maxwellian flux distribution for the most robust results.

BACKGROUND

Force Modeling

To quantify the electrostatic force in such a way that the effects on the debris re-orbiting mission can be fully understood, it is useful to approximate the re-orbit time $t_{\text{re-orbit}}$, which is equal to the time it takes to complete the burn required to achieve ΔV, t_{burn}.

Visualizing the approximate forces acting on the servicer as seen in Figure 1, it is observed that in one direction is the force of thrust F_T as a result of the propulsion system

$$F_T = \frac{m_{\text{prop}} I_{\text{sp}} g_0}{t_{\text{burn}}}, \tag{1}$$

where g_0 is the standard gravity (9.80665 m/s^2), I_{sp} is the specific impulse of the propulsion system, and m_{prop} is the mass of the burned propellant equal to

$$m_{\text{prop}} = m_S \left(1 - \exp \frac{-\Delta V}{I_{\text{sp}} g_0}\right). \tag{2}$$

In the other direction is the electrostatic force F_E acting between the servicer and the target it is towing. This force is calculated by first using the relationship between electric potential ϕ and charge Q between two charged spheres[19,20]

$$\begin{bmatrix} \phi_S \\ \phi_T \end{bmatrix} = k_c \begin{bmatrix} 1/R_S & 1/d \\ 1/d & 1/R_T \end{bmatrix} \begin{bmatrix} Q_1 \\ Q_2 \end{bmatrix} \tag{3}$$

where R_S and R_T are the radii of each sphere, d is the separation distance between them, and k_c is the Coloumb constant equal to 8.988×10^9 (N·m^2)/C^2. Then, F_E can be found using the Coloumb equation

$$F_E = k_c \frac{Q_1 Q_2}{d^2} \tag{4}$$

The radii R_S and R_T are approximated using Equation 5, which provides a simply linear relationship between the mass of the spacecraft and their radii.[21] In this study, $m_S = 500$kg, which allows

*https://thinkorbital.com

it to fall into the category of SmallSat,[22] reducing the cost of fuel for launch and during the reorbit maneuver. The resulting sphere radius is $R_S = 1.5$m. Additionally, $m_T = 4276$kg, which is the average mass of a GEO satellite as of 2014.[23] The resulting sphere radius is $R_T = 4$m.

$$R_{S,T} = 1.152\text{m} + 0.00066350\frac{\text{m}}{\text{kg}}m_{S,T} \tag{5}$$

The net force acting on the servicer is

$$F_{\text{net}} = F_T - F_E \tag{6}$$

Previous research (using a continuous e-beam) shows electrostatic forces between spacecraft on the order of mN or less.[13,14] This poses an interesting challenge for the ET concept. When $F_T = F_E$, the servicer and target can move together with constant velocity ($F_{\text{net}} = 0$). To achieve ΔV to re-orbit, F_T must be greater than F_E ($F_{\text{net}} > 0$). However, if $F_T \gg F_E$, the servicer will accelerate away from the target and F_E will decrease rapidly with separation distance. Thus, F_T must be close to, but very slightly greater than, F_E, if F_E is small. The F_T required to keep the tug ahead of the debris by a fixed separation distance is

$$F_T = \frac{m_S + m_T}{m_T}F_E > F_E \tag{7}$$

where m_S and m_T are the masses of the servicer and target respectively.[4] The small F_T required to maintain F_E means that t_{burn} will be sizable. However, a larger F_E would allow for a larger F_T, and thus a larger F_{net}.

E-Beam Power

Assuming that the ET is equipped with an e-beam with some fixed power specification P, it is of interest to determine if it is optimal to used this power continuously at some given e-beam current I and e-beam voltage V, or if pulsing the e-beam such that I and V are increased during a short time period will maximize the electrostatic force for the same P. We know from the power equation that P is the product of I and V, such that $P = IV$. If the e-beam is pulsed, then the power equation becomes $P = \text{DC} \cdot I_p V_p$, where DC is the duty cycle. To maintain the power specification, I and V must be

$$I_{\text{p}} = \frac{\gamma I}{\sqrt{\text{DC}}} \tag{8}$$

and

$$V_{\text{p}} = \frac{V}{\gamma\sqrt{\text{DC}}} \tag{9}$$

which can be substantially larger than the I and V for the continuous beam depending on DC. A tuning parameter γ is included in these equations. In this study, $\gamma = 1$ because this was found to be generally optimal in previous work and in order to focus on optimizing the electrostatic force with respect to the duty cycle alone. These augmented e-beam properties can cause the magnitude of the potential of both the target and servicer spacecraft to be amplified. This means that the resulting electrostatic force may be increased by using a pulsed beam. The pulsing mechanism used in this study is "on-off" pulsing, meaning that the e-beam will be switched entirely off and back on during one pulsing cycle.

Charging Model

The charging model employed here is based on the one developed by Hammerl and Schaub in Reference 24. As mentioned previously, the charging model assumes fully-conducting spherical spacecraft. It also assumes that the only coupled charging effect is due to the e-beam. Accounting for the secondary and backscattered electrons from the negatively charged target being attracted to the positively charges servicer is left for future work. Moreover, attraction of the plasma particles uses an orbit-limited approximation, which means the flux is calculated as that incident on a sphere of the same potential and depends only on the surface potential.[25] The charging model accounts for the following currents whose equations, dependent on the servicer potential ϕ_S and the target potential ϕ_T, can be found in Reference 24:

- I_e: ambient electron current
- I_p: ambient ion current (assumed to be Hydrogen nuclei)
- I_{beam}: e-beam current
- I_{BS_e}: backscattered electron current due to ambient electrons
- $I_{\text{BS}_{\text{beam}}}$: backscattered electron current due to the e-beam
- I_{SE_e}: secondary electron current due to ambient electron impact
- I_{SE_p}: secondary electron current due to ambient ion impact
- $I_{\text{SE}_{\text{beam}}}$: secondary electron current due to e-beam impact
- I_{PE}: photoelectron current

Thus, the net current on the servicer and the target are each

$$I_{\text{net}} = I_e + I_p + I_{\text{beam}} + I_{\text{BS}_e} + I_{\text{BS}_{\text{beam}}} + I_{\text{SE}_e} + I_{\text{SE}_p} + I_{\text{SE}_{\text{beam}}} + I_{\text{PE}}. \tag{10}$$

The spacecraft are at their equilibrium potentials when $I_{\text{net}} = 0$ for both the servicer and the target. This potential is solved for numerically in Matlab. The time-variant potential is solved for numerically in Matlab using an ordinary differential equation.

Bi-Maxwellian Plasma Environment

Previous research on optimizing the electrostatic tractor in different GEO environments used a single-Maxwellian flux distribution function (FDF)[15,24] or accounted for only one population of particles.[17] However, the plasma environment at GEO is composed of two populations of particles: a cold and dense population of plasmasphere particles and a hotter, more tenuous population of particles injected from the magnetotail. Both populations vary depending on solar storm activity and the local time LT. One way of measuring solar storm activity is by using the planetary K index, or Kp index. Higher values of Kp index correspond to greater geomagnetic activity, with values of $Kp \geq 5$ indicating a solar storm. When the magnetosphere is compressed as a result of solar activity, magnetotail particles are accelerated to high energies and injected into GEO. Magnetotail particles are also accelerated during substorms, and the electron flux is enhanced between local

midnight and dawn as a result of the eastward drift of the injected high energy electrons. The result is a plasma environment that is more accurately represented by a bi-Maxwellian FDF, which accounts for both the cold plasmasphere particles and the hot injected particles. Each population is modeled using a Maxwellian FDF, and their sum is the bi-Maxwellian FDF

$$f(E) = f_1(E) + f_2(E) \tag{11a}$$

$$f_1(E) = n_1 \left(\frac{q_0}{2\pi m T_1}\right)^{1/2} \frac{E}{T_1} \exp\left(-\frac{E}{T_1}\right) \tag{11b}$$

$$f_2(E) = n_2 \left(\frac{q_0}{2\pi m T_2}\right)^{1/2} \frac{E}{T_2} \exp\left(-\frac{E}{T_2}\right) \tag{11c}$$

where q_0 is the unsigned elementary charge, n is the particle density, T is the particle temperature, m is the mass of the particle, and E is energy. The subscript 1 indicates the cold population, and 2 indicates the hot population.

During quiet times, the plasmapause can extend out as far as $L = 7$, fully encompassing GEO at $L = 6.6$, but geomagnetic activity causes the plasmasphere to compress significantly.[26] Within the plasmasphere, electron density decreases exponentially with altitude until reaching the plasmapause, where the electron density is around 100cm^{-3}.[27] The plasmasphere electrons have low energies, generally in the range of 1-10eV.[28] Outside of the plasmapause, the density of these low energy electrons decreases by orders of magnitude.[27] In this paper, the density of the cold electrons at GEO will be modeled as 100cm^{-3} for $Kp = 0$ (no solar activity) and 1cm^{-3} for $Kp = 2, 4$, and 6. This assumption aligns with the equation for the plasmapause location as a function of Kp index in Reference 26. This paper neglects the effects of day/night variations on the electron density, thus, the cold electron density does not vary with local time. The energy of the cold electrons used in this paper is 1eV for all Kp indices.

In this paper, all of the positive ions are assumed to be H nuclei. The densities and energies for the cold ions, hot ions, and hot electrons are taken from Reference 29. The energy of the cold ions is assumed to be 50eV, since the study measures cold ions as all ions with energies between 1 and 100eV. The density of the cold ions varies with Kp index and LT. The hot particle population's densities and energies also vary with both Kp and LT.

FORCE AND TORQUE INCREASES DUE TO DUTY CYCLE

The goal of this work is to maximize the resulting F_E. The first task of this research is to show that the previously presented theory that a pulsed e-beam can increase the magnitude of F_E is true. In this study, the continuous e-beam current is $I = 520\mu$A to keep consistent with Reference 15. Recall that the e-beam voltage V directly corresponds to the e-beam energy E, which has units of electron volts. Then, Equation (9) can be applied to the e-beam energy. The continuous beam energy used here is $E = 40$keV. In the following simulations, the spacecraft separation distance d is 12.5m, center-to-center. The environment parameters used in the following discussion are seen in Table 1. These parameters correspond to $Kp = 6$ and $LT = 4$. This environment was chosen because previous research had shown that the ET performed better in an active environment.[15,17]

Figure 2 illustrates the charging response and the resulting force for duty cycles of 10%, 30%, 50%, 70%, and 90%. The duty cycle percentage corresponds to the amount of time over one pulsing cycle that the e-beam is turned on. The pulsing frequency is set to 1 second as a baseline to allow full

Table 1: Plasma Parameters

Particle	Parameter			
Type	T_1 (eV)	T_2 (eV)	n_1 (cm^{-3})	n_2 (cm^{-3})
Electron	1	2400	1	1.25
Ion	50	8100	0.01	0.95

target discharging. Because we are interested in maximizing the force, let us first analyze Figures 2c and 2d. In the former, it is clearly observed that smaller duty cycles result in greater forces for a short period of time. In other words, as the duty cycle decreases, the force increases, but only for the duration of the pulse. It is then necessary to average the force over the pulsing period to find if the average electrostatic force is greater for a pulsed beam despite experiencing discharging. In Figure 2d, the average force over a pulsing period is plotted as function of the duty cycle. It is evident that as the duty cycle increases, the electrostatic force decreases. Therefore, it can be concluded that using a pulsed beam benefits the attractive force necessary to re-orbit debris.

A couple of interesting considerations come to light after analyzing Figure 2. Because the electrostatic force increases exponentially as the duty cycle decreases, it is a possibility that the average force over a pulsing period will also always increase with a diminishing duty cycle. Charging, however, takes a certain amount of time, as seen in Figures 2a and 2b. At some point, the duty cycle will become so short that the spacecraft will not have time to reach potentials greater than the next largest duty cycle. Thus, the hypothesis is formed that there exists a duty cycle such that the electrostatic force is maximized.

Determining an Optimal Duty Cycle

Using Figure 2 as a baseline, we know that if an optimal duty cycle exists, it will be at most 10%. Therefore, the simulation can be repeated for duty cycles ranging from 1% to 10% to try to numerically determine the duty cycle that minimizes the electrostatic force. Figure 3 shows the simulation repeated for 5 linearly spaced duty cycles from 1% to 10%, with the exception of Figure 3d, which has 50 duty cycle points. It is immediately evident in Figure 3d that the hypothesis that there exists a duty cycle such that the electrostatic force is maximized is true; the force is maximized at 4.489%.

The maximum average force (MAF) as seen in the figure is still on the order of mN, so how much of an effect does this optimization really have on the time to achieve ΔV? The ΔV required to successfully re-orbit the spacecraft can be calculated assuming a Hohmann transfer [30, Chapter 6] from GEO to the graveyard orbit. GEO is located at approximately $r_1 = 42164.1$km from the center of Earth and the graveyard orbit necessitated by laws in place by the Federal Communications Commission is $r_2 = r_1 + 300$km.[31] Then, ΔV is found to be 10.88m/s. This estimate agrees with other calculations for the ΔV to re-orbit GEO spacecraft, which use 11m/s.[32]

The resulting average electrostatic force at each duty cycle is plugged into Equation 7 to obtain the required F_T to maintain a constant separation distance. Then, Equation (1) is rearranged to find t_{burn}. The specific impulse I_{sp} of the propulsion system is 4190s, which is the same I_{sp} as NASA's NEXT ion thruster.[33] Results show the that I_{sp} has a negligible effect on the burn time with such small forces. For a continuous beam, the average electrostatic force is 0.5271mN, which results in a burn time of 93.39 days. Figure 4 shows how the duty cycle affects the burn time to achieve ΔV

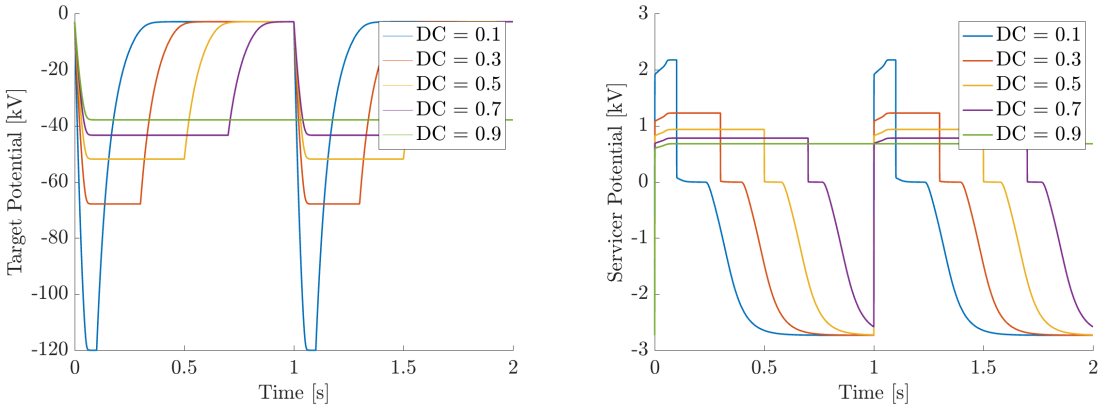

(a) Target potential over time

(b) Servicer potential over time

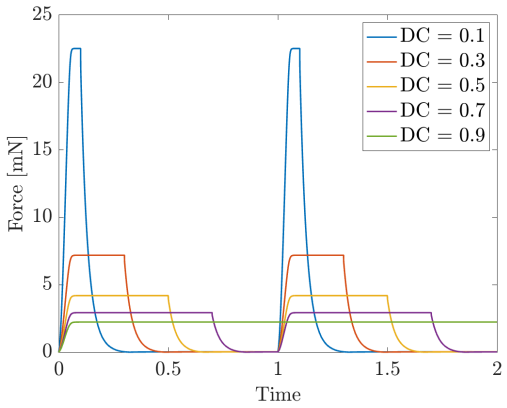

(c) Force over time

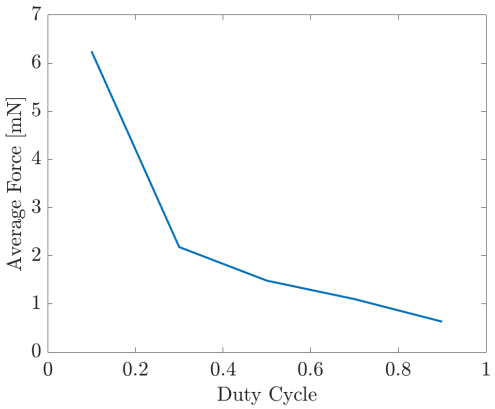

(d) Average force versus duty cycle

Figure 2: Coupled effects of the electrostatic force for duty cycles ranging from 10% to 90%

for duty cycles ranging from 1% to 10%. The maximum force achieved is an order of magnitude stronger than the electrostatic force for the continuous beam, at 10.12mN. This results in a burn time of only 4.865 days, orders of magnitude less than the continuous beam burn time.

Hazard of Field Emission due to High Potentials

When a conducting surface is charged to adequately high potentials such that its electric field is sufficiently enhanced, it may self-emit electrons in a phenomenon called field emission. This emission is modeled using the Fowler-Nordheim (FN) equation[34]

$$J(E) = A\frac{E^2}{\phi}\exp -\frac{B\phi^{3/2}}{E} \tag{12}$$

where J is the emission current density, A and B are constants represented by $A = \frac{1.54\times10^{-6}}{\phi}$, $B = 6.83 \times 10^9$, ϕ is the work function for the material, and E is the electric field at the surface. In this study, the material is assumed to be aluminum, which has a work function $\phi = 4.8$eV.[35] The electric field E can be related the electric potential of the surface V with a simple geometry using[36]

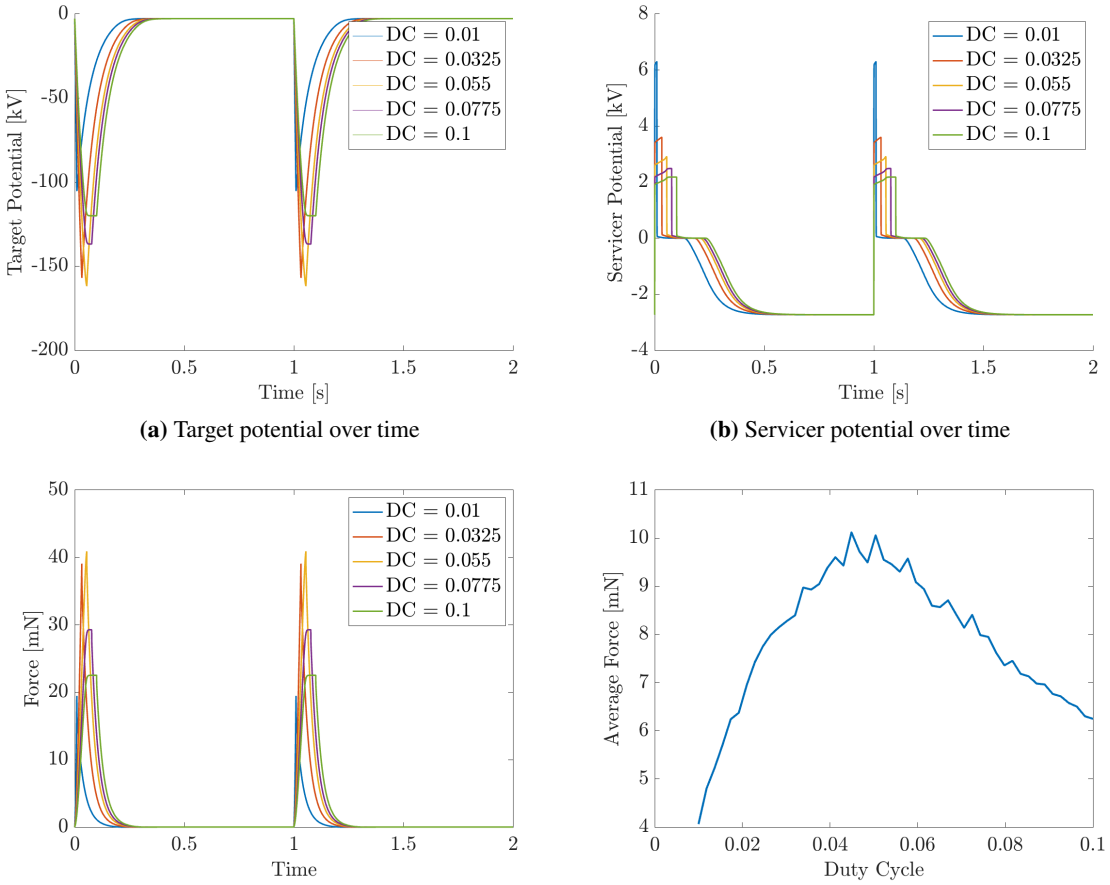

(a) Target potential over time

(b) Servicer potential over time

(c) Force over time

(d) Average force versus duty cycle

Figure 3: Coupled effects of the electrostatic force for duty cycles ranging from 1% to 10%

$$E = \frac{\beta V}{d} \tag{13}$$

where β is the field enhancement factor, which accounts for surface curvature or geometric effects that enhance the local electric field, and d is the separation in meters between the emitter and the counter-electrode. In this study, the spacecraft are assumed to be spherical, so β can be approximated as the ratio of d to the sphere's radius, R_T in this case. Substituting this into Equation 13, we find that for the spherical target,

$$E = \frac{V}{R_T}. \tag{14}$$

Then, substituting Equation 14 into Equation 12, we find

$$J = A\frac{V^2}{R_T^2\phi}\exp -\frac{B\phi^{3/2}R_T}{V}. \tag{15}$$

For an isolated sphere charged to -150kV, the emitted current density as a function of the sphere's radius is show in Figure 5. It is illustrated in the figure that the current density increases exponentially

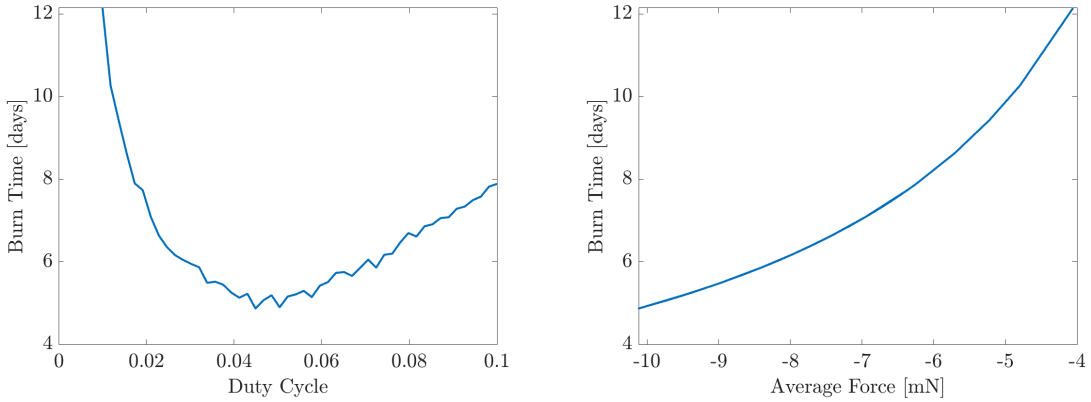

(a) Burn time versus duty cycle

(b) Burn time versus average force

Figure 4: Burn time analysis

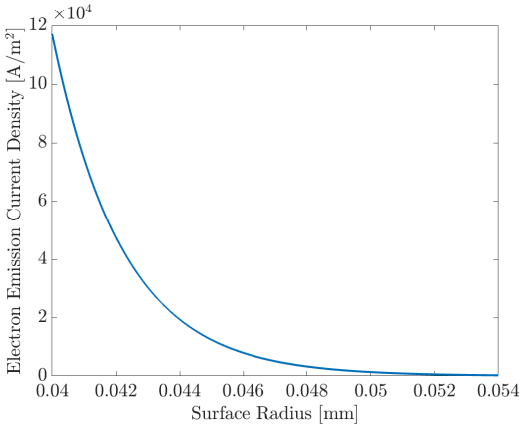

Figure 5: Field emission of an isolated sphere as a function of its radius

as the radius becomes increasingly small. The current density is negligible when the sphere has a radius larger than around 0.052mm, but quickly becomes significant when the radius is smaller than that. The implication of this figure is that surface imperfections, sharp corners, and pointed edges may interfere with the charging of the target. In addition, the electric field of the servicer when in the proximity of these edges would enhance the total electric field, thus increasing the field emission from the target. Risks of field emission include arcing between the spacecraft and limiting the charging potential of the target, thus preventing sufficient electrostatic forces. However, recent experimental trials suggest that increasing the e-beam current may offset the limiting effect of field emission. This is likely because the e-beam current does not govern the maximum charging potential of the target, but instead allows the e-beam to dominate over other charging sources. Thus, the field emission current does not change because the potential of the target does not change, but the e-beam current now more dominant. This study is left for future work.

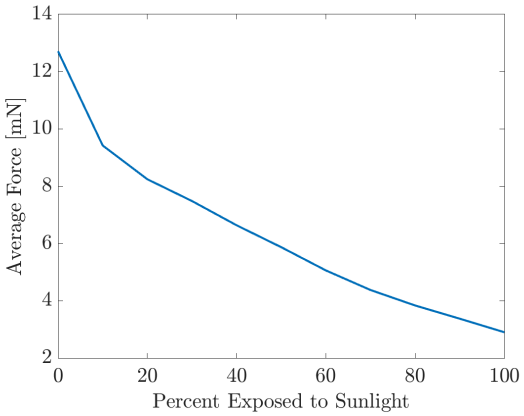

Figure 6: Maximum average force versus percent sun exposure of the projected area

Effect of the Photoelectron Current

The photoelectron current is a positive current on a spacecraft that results from the photons from the sun exciting the electrons on the spacecraft surface. In the previous section, the target was assumed to be in eclipse, so this current was not taken into account. This was in order to provide an adequate picture of the optimal duty cycle. However, in the magnetosphere, the photoelectron current often dominates over the other ambient currents (protons, electrons, and resulting secondary and backscattered currents) [37, Chapter 7]. As a result, GEO spacecraft in sunlight are usually charged up to a few volts positive. GEO spacecraft are rarely in eclipse; the ATS 5 spacecraft, which was in an equatorial geosynchronous orbit, only entered eclipse for 30 minutes each night for a period of 3 to 4 weeks in either side of an equinox.[2] Thus, the photoelectron current is crucial to include when discussing GEO spacecraft.

Figure 6 shows the MAF as a function of the percent of the target spacecraft's projected area surface that is exposed to sunlight. The MAF is found by iterating over the duty cycle to find the one that produces the minimum force in the same process that was used in the previous section. The figure illustrates how increasing the amount of surface exposed to the sun, and thus increasing the photoelectric current, reduces the magnitude of the MAF. The projected area of the servicer is assumed to remain fully exposed to sunlight, so it does not charge negatively due to the environment while the e-beam is powered off. This figure essentially simulates how the servicer's shadow on the target affects the electrostatic force between them. When the target's projected area is fully exposed to sunlight, the MAF is 2.900mN, compared to 12.71mN in eclipse. However, the pulsed beam in full sun still performs significantly better than the continuous beam in eclipse (MAF = 0.5271mN).

To further emphasize the effectiveness of the pulsed electron beam, Figure 7 shows the charging and force responses for duty cycles of 10%, 30%, 50%, 70%, and 90% in full sunlight. Figure 7a shows that the target does not charge adequately negative for the duty cycles greater than 10%. While there is an initial pulse for the 30% duty cycle, this is because the e-beam current acts more quickly on the spacecraft than the environment. Thus, after the first pulse, the effect of the environment is in full effect. The lack of charging for higher duty cycles demonstrates the dominance of the photoelectric current compared to the other currents, including the e-beam current. As a result, the force is consistently near-zero for the higher duty cycles, as seen in Figure 7c. Therefore, in order to even generate an electrostatic force with spacecraft of these sizes in this environment, the pulsed

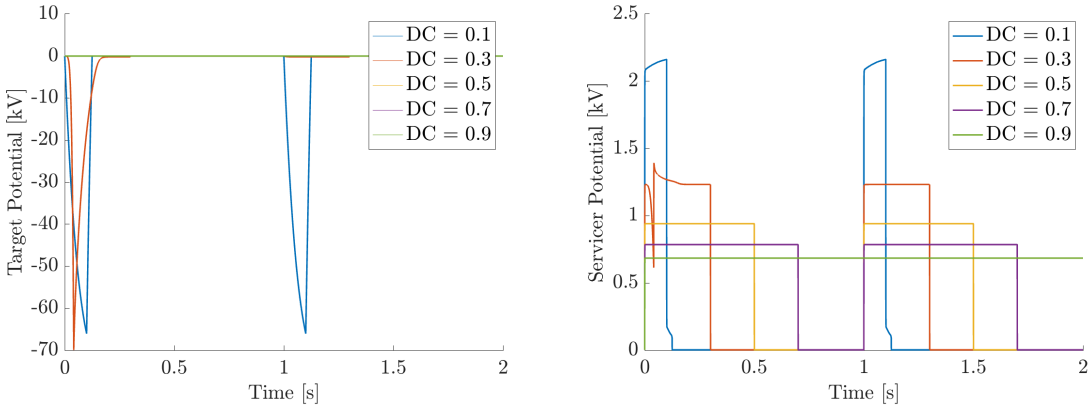

(a) Target potential over time

(b) Servicer potential over time

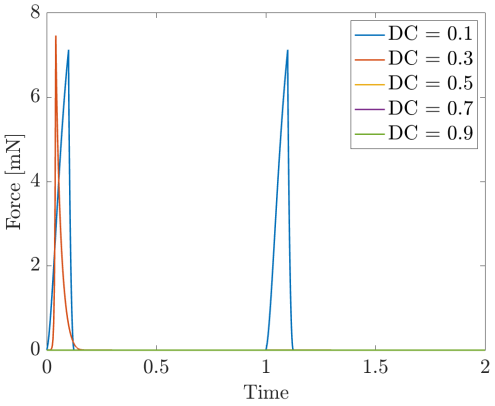

(c) Force over time

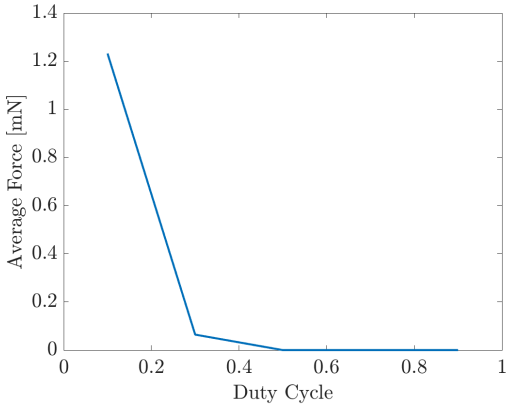

(d) Average force versus duty cycle

Figure 7: Coupled effects of the electrostatic force for duty cycles ranging from 10% to 90% in full sunlight

electron beam must be employed.

EFFECT OF THE NOMINAL GEO ENVIRONMENT ON PEAK FORCE

The plasma environment in GEO is constantly changing as a result of geomagnetic storms and substorms, which accelerate protons and electrons to high energies and inject them into synchronous altitudes. In the previous sections, the plasma parameters were those shown in Table 1, which correspond to $Kp = 6$ and $LT = 4$. As the plasma environment varies, it is of interest to investigate the impact the changing environment has on the electrostatic force enhancement obtained by pulsing the e-beam.

Figure 8a shows the MAF as a function of the Kp index at $LT = 4$. The Kp index varies from $Kp = 0$ to $Kp = 6$. In reality, the Kp scale goes up to $Kp = 9$, but less than 5% of days per 11-year solar cycle reach values greater than $Kp = 6$.[38] In addition, we can recognize the pattern and make adequate predictions about the force enhancement during more severe solar storms. The key observation is that the MAF increases with K_p index. In other words, the pulsed electron beam performs better during active periods, which corroborates results from previous research.[15,17] The

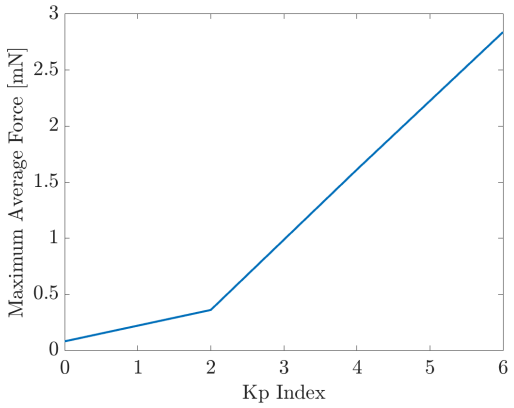

(a) Kp index versus minimum average force

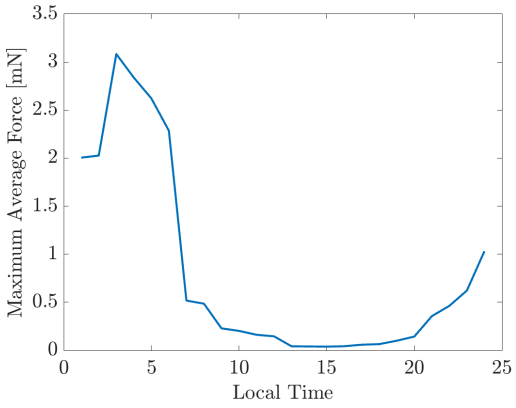

(b) Local time versus minimum average force

Figure 8: Effect of a changing environment on minimum average force in sunlight

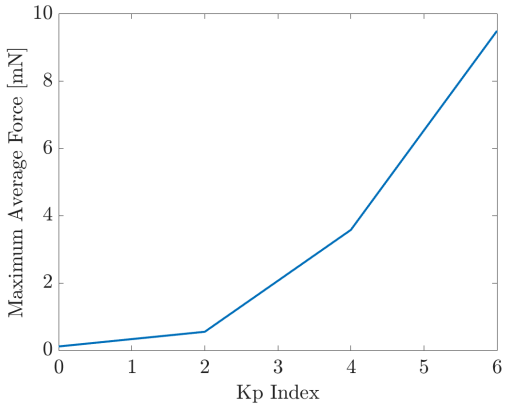

(a) Kp index versus minimum average force

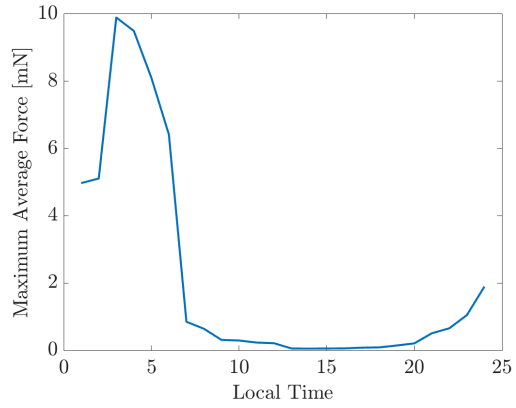

(b) Local time versus minimum average force

Figure 9: Effect of a changing environment on minimum average force in eclipse

data in Figure 8a includes the photoelectron current at full sun exposure. At $K_p = 0$, the MAF is near zero, which is likely a result of the currents from the cold, dense plasma that is present dominating the electron beam current. The duty cycles used to find the MAF ranged from 1% to 10%, and it was not tested if perhaps an even smaller duty cycle may have performed better. This seems unlikely, though, considering the time required to fully charge up the spacecraft.

Figure 8b, which shows the minimum average force as a function of LT at $Kp = 6$, follows the expected pattern based on the results of Figure 8a. Around local midnight ($LT = 24$) the MAF decreases quickly, peaking during the early morning hours. Then, the plasmasphere particles move back into GEO and the cold, dense particles quickly dominate over the electron beam current. The near-zero forces seen in both Figure 8b and 9b, which shows the same results but in eclipse, indicate that geomagnetic activity is essential for ET function at the current and voltage used here. However, stronger e-beams may provide the currents and energies necessary to function in even quiet environments.

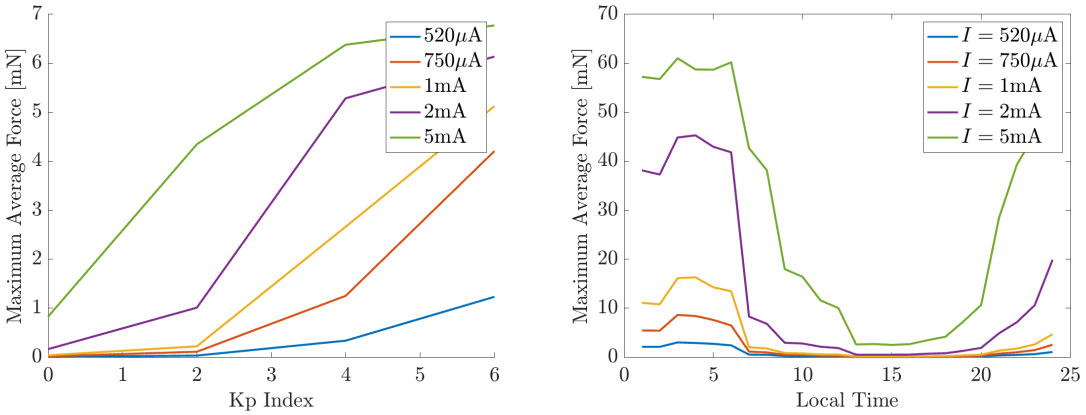

(a) Maximum average force as a function of Kp

(b) Maximum average force as a function of LT

Figure 10: Effect of changing e-beam current for duty cycles from 1% to 10%

EFFECT OF ELECTRON BEAM POWER ON PEAK FORCE IN QUIET ENVIRONMENTS

To combat the cold plasmasphere particles that mitigate active charging during quiet periods in GEO, e-beams with greater fixed powers are explored. In the previous scenarios, the continuous beam parameters were fixed at $I = 520\mu$A and $E = 40$keV, which is equivalent to a beam power of $P = 20.8$W. At this power setting, the electrostatic force was near-zero during quiet periods. The potential of the target spacecraft is limited by the pulsed energy of the e-beam. For example, at a duty cycle of 1%, the pulsed energy of the e-beam is $40\text{keV}/\sqrt{0.01} = 400$keV. Thus, the target could charge to a maximum of 400V. However, for such small duty cycles, the time it takes for the spacecraft to charge prevents it from reaching its maximum potential in the period that the e-beam is turned on. The spacecraft can be charged more quickly by increasing the e-beam current.

Figure 10 shows the effect of increasing the continuous beam current in the varying bi-Maxwellian environment for duty cycles ranging from 1% to 10% and a pulsing frequency of 1Hz. In Figure 10a, the local time is fixed at $LT = 4$, and in Figure 10b, the Kp index is fixed at $Kp = 6$. The spacecraft are exposed to full sunlight. The results show how increasing the e-beam current allows the electrostatic force to grow as a result of the faster charging induced by higher currents. The maximum charging potential remains constant for each duty cycle, but the spacecraft is able to reach higher potentials in the period that the e-beam is turned on because it charges quicker. For example, in Figure 10b, even at its minimum at $LT = 13$, the MAF for the 5mA (continuous current value) e-beam is 2.591mN. This value is nearly 5 times greater than the result for the continuous e-beam at 520μA in optimal environmental conditions and in eclipse. In Figure 10a, it is seen that at $Kp = 0$, charging is still difficult even with higher currents. However, the 5mA e-beams still produces a MAF of 0.8261mN, which is still greater than the optimal continuous case. At higher Kp indexes, each more powerful e-beam quickly overcomes the environment and performs better than the next highest power setting. Thus, using more powerful e-beams, specifically with greater current allowances, is a promising solution to overcoming environmental challenges.

Figure 11 illustrates the charging and force responses of the spacecraft at duty cycles ranging from 1% to 10% at a pulsing frequency of 1Hz for a continuous beam current of $I = 5$mA in sunlight. It is immediately evident from Figure 11d that the result is not optimized. At a the duty cycle of

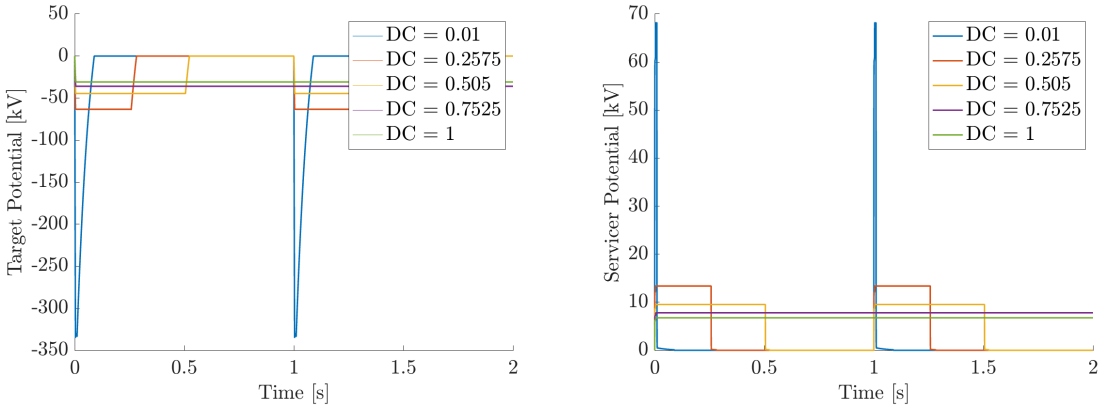

(a) Target potential over time

(b) Servicer potential over time

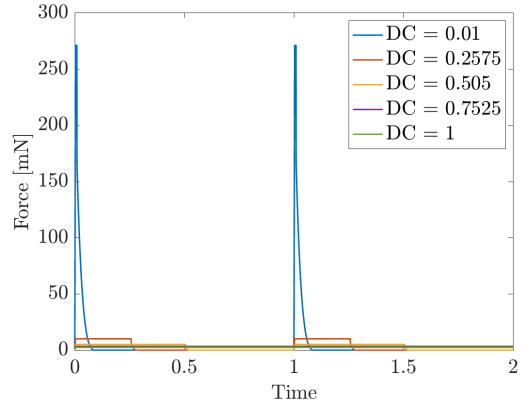

(c) Force over time

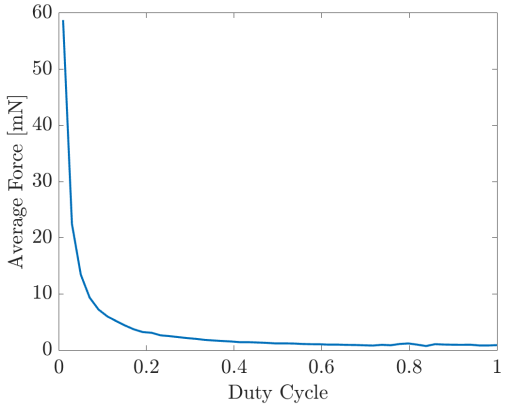

(d) Average force versus duty cycle

Figure 11: Coupled effects of the electrostatic force for duty cycles ranging from 1% to 10% at $I = 5\text{mA}$

1%, the beam energy is $40\text{keV}/\sqrt{0.01} = 400\text{keV}$. Thus, it is also evident that the spacecraft does not have time to charge to its maximum potential (400kV) in the time that the e-beam is powered on. This means that for smaller duty cycles, the spacecraft will also not charge to its maximum possible potential. It was previously concluded that an optimal duty cycle will exist such that the force is maximized. However, to decrease the duty cycle would continue to increase the e-beam power required. Commercially available e-beams have powers of up to only 100keV [*], with those used in space applications at only 20keV. Thus, it is not practical to explore duty cycles that would require these exceedingly high energy levels. Likewise, this configuration requires a pulsed e-beam current of $5\text{mA}/\sqrt{0.01} = 50\text{mA}$, where commercial e-beams allow currents up to 20mA and ones currently in development allow currents up tot 30mA. The e-beam limitations will be a challenge for overcoming environmental charging obstacles in application.

[*] https://www.kimballphysics.com/product/egh-8201-egps-8201/

CONCLUSION

In this paper, the effects of pulsing an e-beam were studied in the context of the electrostatic tractor concept. The goal was to maximize the electrostatic force to generate to the greatest attractive force between the servicer and target spacecraft. It was found that decreasing the duty cycle decreases the average electrostatic force until the duty cycle becomes small enough such that the target cannot fully charge in the time that the e-beam is turned on. As a result, the electrostatic force decreases when the duty cycle decreases beyond an optimal value. The optimal duty cycle results in a force that may be orders of magnitude greater than that of a continuous beam. The burn time to achieve the ΔV required to transfer to a graveyard orbit is then also orders of magnitude less than that using a continuous beam. Overall, the pulsed electron beam presents a promising solution to optimizing debris removal in GEO. However, some limitations still exist. While in an eclipse, the target spacecraft may charge to over -100kV, which poses a risk of field emission. Field emission presents risks such as limiting the charging potential of the target or even causing arcing between spacecraft. This topic is unexplored in the context of active spacecraft charging and is left for future work. During quiet periods in GEO, the spacecraft are limited in their charging by the very cold and more dense plasmasphere particles that may extend into the GEO regime. To over come this obstacle, more powerful electron beams are explored. However, commercially available electron beams that currently exist have maximum beam energies and currents that may prevent charging to the necessary potentials to overcome the changing environment.

ACKNOWLEDGMENT

The authors would like to thank Julian Hammerl for his spacecraft charging model and his guidance using the pulsed beam simulation. He was a significant asset to the completion of this project. This work was supported by the U.S. Air Force Office of Scientific Research under grant FA9550-23-S-0570.

REFERENCES

[1] S. T. Lai, *Fundamentals of Spacecraft Charging*. Princeton University Press, Oct. 2011, 10.2307/j.ctvcm4j2n.

[2] S. E. DeForest, "Spacecraft Charging at Synchronous Orbit," *Journal of Geophysical Research*, Vol. 77, 1972.

[3] R. C. Olsen, "Record charging events from Applied Technology Satellite 6," *Journal of Spacecraft and Rockets*, Vol. 24, Jul. 1987, pp. 362–366, 10.2514/3.25925.

[4] H. Schaub and J. D. F. Moorer, "Geosynchronous large debris reorbiter: Challenges and prospects," *The Journal of Astronautical Sciences*, Vol. 59, 2012, pp. 161–176.

[5] E. Hogan and H. Schaub, "Impacts of Tug and Debris Sizes on Electrostatic Tractor Charging Performance," *Advances in Space Research*, Vol. 55, 2015, pp. 630–638.

[6] H. Schaub and Z. Sternovsky, "Active space debris charging for contactless electrostatic disposal maneuvers," *Advances in Space Research*, Vol. 53, 2014, pp. 110–118.

[7] E. H. Trevor Bennett, Daan Stevenson and H. Schaub, "Prospects and challenges of touchless electrostatic detumbling of small bodies," *Advances in Space Research*, Vol. 56, 2015, pp. 557–568.

[8] T. Bennett and H. Schaub, "Touchless Electrostatic Three-dimensional Detumbling of Large Axisymmetric Debris," *Journal of Astronautical Science*, Vol. 62, 2015, p. 233–253.

[9] T. Bennett and H. Schaub, "Contactless Electrostatic Detumbling of Axi-Symmetric GEO Objects with Nominal Pushing or Pulling," *Advances in Space Research*, Vol. 62, 2018, p. 2977–2987.

[10] D. Stevenson, "Electrostatic spacecraft rate and attitude control—Experimental results and performance considerations," *Acta Astranautica*, Vol. 119, 2016, pp. 22–33.

[11] V. Aslanov, "Detumbling Attitude Control Analysis Considering an Electrostatic Pusher Configuration," *Journal of Guidance, Control, and Dynamics*, Vol. 2, 2019, pp. 900–909.

[12] K. Champion and H. Schaub, "Electrostatic Potential Shielding in Representative Cislunar Regions," *IEEE Transactions on Plasma Science*, Vol. 51, 2023, p. 2482–2500.

[13] J. Hammerl and H. Schaub, "Reduced Order Spacecraft Charging Models for Electrostatic Proximity Operations," *IEEE Transactions on Plasma Science*, submitted.

[14] A. Haft and H. Schaub, "Electrostatic Tractor Effectiveness in a Non-Maxwellian GEO Plasma Environment," *AAS Astrodynamics Specialist Conference*, August 2024.

[15] E. A. Hogan and H. Schaub, "Impacts of Hot Space Plasma and Ion Beam Emission on Electrostatic Tractor Performance," *IEEE TRANSACTIONS ON PLASMA SCIENCE*, Vol. 43, 2015.

[16] H. Schaub, L. E. Z. Jasper, P. V. Anderson, and D. S. McKnight, "Cost and risk assessment for spacecraft operation decisions caused by the space debris environment," *Acta Astranautica*, Vol. 113, 2015, pp. 66–79.

[17] J. Hughes and H. Schuab, "Prospects of Using a Pulsed Electrostatic Tractor With Nominal Geosynchronous Conditions," *IEEE Transactions on Plasma Science*, Vol. 45, No. 8, 2017.

[18] J. Hughes and H. Schaub, "Orbital And Storm Time Analysis Of The Pulsed Electrostatic Tractor," *European Conference on Space Debris*, April 2017.

[19] W. R. Smythe, *Static Dynamic Electricity, 3rd Edition*. McGraw Hill, 1968.

[20] D. Stevenson and H. Schaub, "Multi-sphere method for modeling spacecraft electrostatic forces and torques," *Advances in Space Research*, 2013.

[21] H. Schaub and L. E. Z. Jasper, "Orbit Boosting Maneuvers for Two-Craft Coulomb Formations," *Journal of Guidance, Control, and Dynamics*, 2013.

[22] "Smallsats by the numbers," 2020. https://brycetech.com/reports/report-documents/Bryce$_Smallsats_2020.pdf$.

[23] B. Ostrove, "Average Commercial Communications Satellite Launch Mass Declines, Again," *Defense and Security Monitor*, 2015.

[24] J. Hammerl and H. Schaub, "Coupled Spacecraft Charging Due to Continuous Electron Beam Emission and Impact," *Journal of Spacecraft and Rockets*, 2024.

[25] V. Davis, B. Gardner, and M. Mandell, "Nascap-2k version 4.3 users manual," *Leidos Holdings San Diego, CA, USA, Tech. Rep. AFRL-RVPS-TR-2017-0002*, 2016.

[26] V. Pierrard, E. Botek, J.-F. Ripoll, *et al.*, "Links of the Plasmapause With Other Boundary Layers of the Magnetosphere: Ionospheric Convection, Radiation Belt Boundaries, Auroral Oval," *Frontiers in Astronomy and Space Sciences*, Vol. 8, 2021.

[27] H. Laakso, O. Opgenoorth, J. Wygant, *et al.*, "Electron Density Distribution in the Magnetosphere," *Correlated Phenomena at the Sun, in the Heliosphere and in Geospace. 31st ESLAB Symposium*, 1997.

[28] D. J. Williams, "Dynamics of the earth's ring current: Theory and observation," *Space Science Reviews*, Vol. 42, 1985, pp. 375–396.

[29] M. H. Denton, M. F. Thomsen, H. Korth, S. Lynch, J. C. Zhang, and M. W. Liemohn, "Bulk plasma properties at geosynchronous orbit," *Journal of Geophysical Research: Space Physics*, 2005.

[30] D. A. Vallado, *Fundamentals of Astrodynamics and Applications*. Microcosm Press and Kluwer Academic Publishers, 2001.

[31] P. de Selding, "FCC Enters Orbital Debris Debate," *Space News Business Report*, 2004.

[32] F. Paganucci, G. Saccoccia, and F. Scortecci, "Method for re-orbiting a dual-mode propulsion geostationary spacecraft," 29 1997. US Patent 5651515A.

[33] "Gridded Ion Thrusters (NEXT-C): NEXT Ion Engine Test Firing," https://www1.grc.nasa.gov/space/sep/gridded-ion-thrusters-next-c/.

[34] R. H. Fowler and L. Nordheim, "Electron Emission in Intense Electric Fields," *Proceedings of the Royal Society A: Mathematical, Physical and Engineering Sciences*, Vol. 119, 1928, pp. 173–181.

[35] H. B. Michaelson, "The Work Function of the Elements and its Periodicity," *Journal of Applied Physics*, Vol. 48, 1977.

[36] R. G. Forbes, "Field Emission: New Theory for the Derivation of Emission Area from a Fowler-Nordheim Plot," *Journal of Vacuum Science Technology B: Microelectronics and Nanometer Structures Processing, Measurement, and Phenomena*, Vol. 19, 2001, pp. 1280–1286.

[37] S. T. Lai, *Fundamentals of Spacecraft Charging*. Princeton University Press, 2012.

[38] Space Weather Prediction Center, "NOAA Space Weather Scales," https://www.swpc.noaa.gov/noaa-scales-explanation.